Cryogenic testing of the 2.1 GHz five-cell superconducting RF cavity with a photonic band gap coupler cell

Cite as: Appl. Phys. Lett. **108**, 222603 (2016); https://doi.org/10.1063/1.4953204
Submitted: 25 April 2016 . Accepted: 21 May 2016 . Published Online: 02 June 2016

Sergey A. Arsenyev, Richard J. Temkin, W. Brian Haynes, Dmitry Yu. Shchegolkov, Evgenya I. Simakov, Tsuyoshi Tajima, Chase H. Boulware, Terrence L. Grimm, and Adam R. Rogacki

Cryogenic testing of the 2.1 GHz five-cell superconducting RF cavity with a photonic band gap coupler cell

Sergey A. Arsenyev,[1,a)] Richard J. Temkin,[1] W. Brian Haynes,[2] Dmitry Yu. Shchegolkov,[2] Evgenya I. Simakov,[2] Tsuyoshi Tajima,[2] Chase H. Boulware,[3] Terrence L. Grimm,[3] and Adam R. Rogacki[3]

[1]*Massachusetts Institute of Technology, 77 Mass. Ave., Cambridge, Massachusetts 02139, USA*
[2]*Los Alamos National Laboratory, PO Box 1663, Los Alamos, New Mexico 87545, USA*
[3]*Niowave, Inc., 1012 North Walnut Street, Lansing, Michigan 48906, USA*

(Received 25 April 2016; accepted 21 May 2016; published online 2 June 2016)

We present results from cryogenic tests of the multi-cell superconducting radio frequency (SRF) cavity with a photonic band gap (PBG) coupler cell. Achieving high average beam currents is particularly desirable for future light sources and particle colliders based on SRF energy-recovery-linacs (ERLs). Beam current in ERLs is limited by the beam break-up instability, caused by parasitic higher order modes (HOMs) interacting with the beam in accelerating cavities. A PBG cell incorporated in an accelerating cavity can reduce the negative effect of HOMs by providing a frequency selective damping mechanism, thus allowing significantly higher beam currents. The multi-cell cavity was designed and fabricated of niobium. Two cryogenic (vertical) tests were conducted. The high unloaded Q-factor was demonstrated at a temperature of 4.2 K at accelerating gradients up to 3 MV/m. The measured value of the unloaded Q-factor was 1.55×10^8, in agreement with prediction. *Published by AIP Publishing.* [http://dx.doi.org/10.1063/1.4953204]

In the last decade, there has been significant interest in high-current energy-recovery-linac (ERL) driver accelerators for light sources[1–4] and electron-proton colliders.[5] However, the beam current in ERLs is limited by the beam break-up (BBU) instability, which comes as a result of interaction of the beam with parasitic electromagnetic modes in accelerating structures.[6,7] This effect is caused primarily by the modes of dipole or quadrupole nature with frequencies above the accelerating mode's frequency. These modes are called higher order modes (HOMs).

Consideration of the BBU instability becomes especially important given the fact that many ERLs[1–5] rely on superconducting radio-frequency (SRF) accelerating cavities that are the natural choice for operation in a continuous wave (CW) mode.[8] Once HOMs are excited in superconducting cavities, they can oscillate for a long time with very high Q-factors due to extremely low losses in the walls of the cavities.

Photonic band gap (PBG) cells are known for good HOM suppression due to their intrinsic frequency selectivity, which can be used to confine the accelerating mode but not the HOMs.[9] The SRF PBG prototype resonator, operating at the frequency of 11 GHz, was designed and fabricated about two decades ago.[10] The resonator's Q-factor was shown to be at least 1.2×10^6 at the temperature of 4.8 K. Later, the first room temperature multi-cell PBG accelerating cavity was designed and tested with an electron beam at MIT.[11] This was a travelling wave copper structure operating at 17 GHz.

Advances in PBG technology for room-temperature accelerators revived interest in superconducting PBG cavities. A superconducting PBG resonator design was proposed in Ref. 12. A prototype, operating at the frequency of 16 GHz, was tested at cryogenic temperatures and showed $Q = 1.2 \times 10^5$ limited by radiation losses. Recently, several single SRF PBG cells operating at 2.1 GHz were fabricated and tested at Los Alamos National Laboratory (LANL).[13,14] The results showed that high accelerating gradients (18 MV/m at the temperature of 4 K) and high unloaded Q-factors (4×10^9 at the temperature of 1.9 K) could be achieved in the PBG cells.

In this paper, we present cryogenic tests of the multi-cell accelerating SRF cavity that incorporates a PBG cell. Similar to the single cells tested at LANL, this cavity operates at the frequency of 2.1 GHz. The cavity has five cells: four elliptical cells and one PBG cell in the middle (Figure 1). Three waveguides are attached to the periphery of the PBG cell. One of the waveguides has a larger cross-section, and is used both as an HOM coupler and as the fundamental power coupler (FPC). The smaller waveguides are HOM couplers. The PBG rod located closest to the FPC was removed to allow stronger

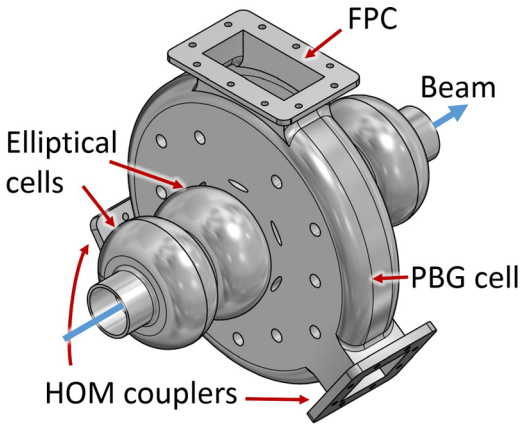

FIG. 1. Drawing of the 2.1 GHz 5-cell SRF cavity with the PBG cell in place of one of the elliptical cells.

a)arsenyev@mit.edu

coupling to the accelerating mode. The cavity dimensions and accelerating properties are listed in Table I. Detailed discussion of the cavity's design and HOM damping properties can be found in Refs. 15 and 16.

The cavity was fabricated of niobium (RRR $\geq$ 240) at Niowave, Inc. The fabrication process is described in Refs. 15 and 16. The first cryogenic vertical test was conducted at LANL. The three waveguides were covered with niobium plates for the purpose of this experiment. Coupling to the cavity was done through a coaxial pickup probe and an adjustable coaxial drive probe, mounted in the opposite beam pipes of the cavity. The probes were designed to form a 50 Ω line with the beam pipe to minimize reflections at the cable connections. Adjustability was provided by a bellows that could be squeezed or extended to vary the coupling strength to the cavity's mode. A 200 W travelling wave tube (TWT) amplifier was used to provide power at 2.1 GHz. The cavity was lowered into a cryostat equipped with a magnetic field compensating coil that reduced the ambient magnetic field at the location of the cavity to <10 mG.[17]

In the test, we measured Q-factors and field levels for different monopole "passband" modes in the cavity, ranging in the frequency from 2.028 to 2.105 GHz. The 5-cell cavity has 5 passband modes that are classified according to their phase advance over the length of one cell: from $\pi/5$ to π. Electric field along the central axis for different modes is plotted in Figure 2. The $\pi/5$ mode was not excited in this experiment due its relatively weak coupling to the drive probe.

Expected unloaded quality factors Q_0 at the temperature of 4.0 K (the helium boiling temperature corresponding to atmospheric pressure of 600 Torr at LANL) are listed in the second column of Table II. These expectations are based on the geometry constants G, simulated in Ansys HFSS,[18] and the surface resistance R_s which can be divided into contributions from the BCS model R_{BCS} and the residual resistance R_0.

The value of R_{BCS} was calculated using the following formula from Ref. 19:

$$R_{BCS} = 2 \times 10^{-4} \frac{1}{T} \left(\frac{f}{1.5}\right)^2 \exp\left(-\frac{17.67}{T}\right), \qquad (1)$$

where f is the frequency in GHz and T is the temperature in K. R_{BCS} was estimated to be 1.189 $\mu\Omega$ at the temperature of 4.0 K. We also estimated the residual resistance due to magnetic flux trapped in the walls of the cavity. Using an empirical formula from Ref. 20, we found $R_0 \approx 18$ nΩ $\ll R_{BCS}$ for the measured value of DC magnetic field. Hence, the residual resistance contribution to the total surface resistance was neglected.

TABLE I. Dimensions and accelerating properties of the 5-cell cavity with a PBG cell.

Cavity length	35.1 cm
Inner beam pipe radius	2.49 cm
Inner diameter of the elliptical cells	12.6 cm
Inner diameter of the PBG cell	32.4 cm
Outer diameter of the round PBG rods	1.78 cm
Spacing between the PBG rods	5.87–5.94 cm
Frequency f_0	2100 MHz
Shunt impedance R/Q	515 Ω
Geometry constant G	265 Ω
Peak surface electric field ratio E_{peak}/E_{acc}	2.65
Peak surface magnetic field ratio B_{peak}/E_{acc}	4.48 $mT/(MV/m)$

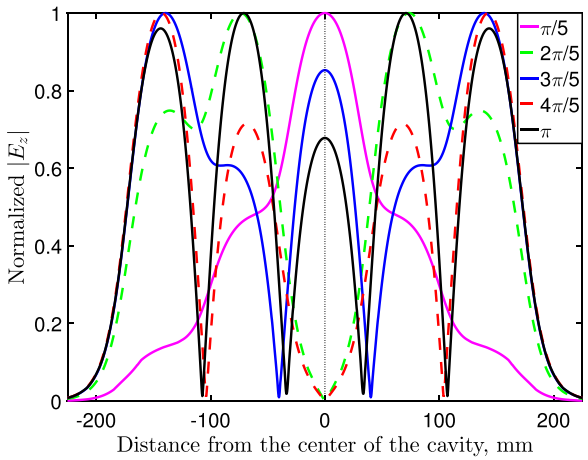

FIG. 2. Simulated electric field profiles along the central axis for the 5 passband modes of the 5-cell cavity.

The third column in Table II lists the values of Q_0, obtained from the pulsed and CW measurements. Q_0 for the $2\pi/5$ and the $4\pi/5$ modes were close to the expected values, however Q_0 for the $3\pi/5$ and the π modes were about two orders of magnitude lower than the expected values. The problem of low Q prevented coupling to the $3\pi/5$ and the π modes and did not allow to feed any significant power into the cavity at these modes. Therefore, high electric and magnetic fields were only achieved in the $2\pi/5$ and the $4\pi/5$ modes, eventually limited by the available RF power.[16] Maximum achieved surface electric fields are listed in the last column of Table II.

Next, the cryostat was pumped down to the pressure of 26 Torr, corresponding to the temperature of 2.04 K, but coupling to the π mode did not improve. This indicated that the mode's Q_0 was limited by some losses of non-superconducting nature.

After the first experiment, effort was put into understanding the cause of the unusually high losses for the π and the $3\pi/5$ modes. The fact that only the modes with significant fields in the center cell (Figure 2) had low Q_0, indicated that the source of the losses was located in the PBG cell. At the same time, the fact that no unusual losses were observed in the experiments with single PBG cells without attached waveguides indicated that the problem might have been in

TABLE II. Low-field Q_0 and peak surface electric fields measured at 4.0 K in the first cryogenic test at LANL.

Mode	Q_0 at 4.0 K, simulated	Q_0 at 4.0 K, measured	E_{surf}^{peak}, measured
$\pi/5$	1.83×10^8	…	…
$2\pi/5$	2.27×10^8	2.2×10^8	17.5 MV/m
$3\pi/5$	2.07×10^8	9.3×10^5	…
$4\pi/5$	2.27×10^8	2.7×10^8	29.1 MV/m
π	2.15×10^8	1.6×10^6	…

the waveguide covers. Among the waveguides, the FPC seemed to be the most likely cause of the problem because fields in it were much higher than in the HOM couplers.

The cross-section view of the FPC cover is shown in Figure 3. Given previous experience at Niowave, Inc., it was chosen to use the following design: clamped niobium-to-niobium contact provided an RF seal, as in Ref. 21, and a hexagonally shaped aluminum gasket provided a vacuum seal, as in the "diamond" gasket design.[22]

A series of room temperature experiments were conducted to verify that the problem was indeed with the FPC joint. A "trapped" waveguide mode was excited in the FPC by specially made long antennas. The test showed that the trapped mode had an unusually low Q factor even at room temperature, proving the hypothesis of the lossy FPC joint. The losses were a result of the cover plate only touching the flange at a few points, as opposed to a uniform contact along the entire perimeter.

To solve the problem, the shape of the niobium plate was modified to improve the RF contact as the plate is pressed to the cavity. An adjustment was also made to the depth of the groove for the aluminum gasket. Careful examination of mechanical stresses was done to make sure that both niobium and aluminum gaskets are crushed equally. The improved design was tested at room temperature, demonstrating that the Q factor of the trapped mode was restored to its expected value. The joints on the HOM couplers were also replaced with the improved design.

After the modifications were made, the cavity underwent another surface treatment that consisted of buffered chemical polish (BCP) flash etching and high-pressure rinsing. The cavity was re-tested at Niowave in December of 2015. Besides the improved joint, the cavity was also welded into a titanium helium vessel, as can be seen in Figure 4. Addition of the helium vessel brought the cavity a step closer towards an accelerator-ready cryomodule. The helium vessel also eliminated the need for a large helium tank used in the previous cryogenic test.

Similar to the first experiment at LANL, coupling to the cavity was done through drive and pickup probes, located in

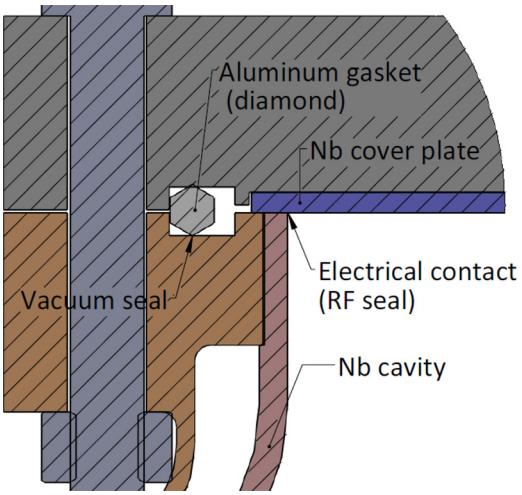

FIG. 3. Cross-section of the FPC waveguide cover (only one side is shown). The niobium-to-niobium contact provided an RF seal, and the aluminum gasket provided a vacuum seal.

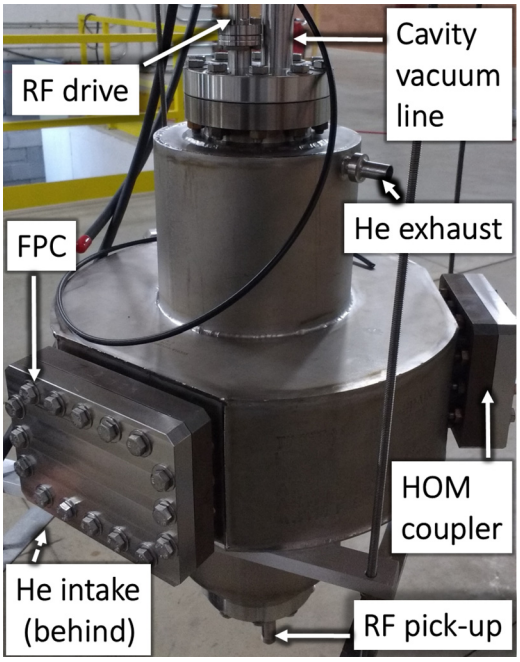

FIG. 4. A photograph of the 2.1 GHz 5-cell cavity in the helium vessel ready to be placed in a cryostat in preparation for the second cryogenic test.

the beam pipes. This time the probes were non-adjustable and did not match the 50 Ω impedance of the coaxial lines. The drive antenna was designed to be fairly overcoupled (target coupling $\beta = 5$ for the accelerating mode) in order to have more RF power available for possible multipacting processing. A solid state 100 W amplifier was chosen as the 2.1 GHz RF power source.

No baking was performed prior to the cryotest. The cavity in the helium vessel was placed in the vacuum region of a cryostat. A μ-metal shield was used to bring the ambient magnetic field in the cryostat down to 7 mG.

Cavity cooldown proceeded smoothly and without interruption, taking approximately 4 h to reach the superconducting transition. Cavity vacuum was maintained below 10^{-8} Torr. Unless otherwise noted, measurements described below were conducted with the helium boiling at atmospheric pressure of 760 Torr (T = 4.2 K). A temperature sensor attached to upper part of the helium vessel served as a helium level meter. A rise in temperature indicated that the cavity was not fully covered in helium, and the flow of helium would be increased.

Measured pulse decay times were used to calculate the loaded Q-factors Q_L at low power levels for all the 5 passband modes (Table III). The obtained values of Q_L for most

TABLE III. Comparison between the low-field Q_L measured at the temperature of 4.2 K and the expected values of Q_L based on the estimated Q_{ext} and Q_0 for different modes.

Mode	Q_{ext}, simulated	Q_0, simulated	Q_L, simulated	Q_L, measured
$\pi/5$	6.45×10^8	1.50×10^8	1.21×10^8	1.19×10^8
$2\pi/5$	3.87×10^7	1.87×10^8	3.21×10^7	5.54×10^7
$3\pi/5$	2.92×10^7	1.72×10^8	2.50×10^7	4.60×10^7
$4\pi/5$	1.95×10^7	1.87×10^8	1.77×10^7	1.72×10^7
π	2.84×10^7	1.81×10^8	2.45×10^7	2.50×10^7

of the modes agree well with the expectations based on simulated Q_{ext} and the BCS model for the surface resistance (Equation (1)). The residual resistance was neglected, as before. The $\pi/5$ mode was the only undercoupled passband mode due to its low fields in the end cells, as can be seen in Figure 2. Therefore, for the $\pi/5$ mode $Q_L \approx Q_0$, and comparing its Q_L to the expectation was particularly interesting as it could have revealed the presence of the anomalous losses observed before. The fact that the measured Q_L for the $\pi/5$ mode agreed well with the expectation, together with the fact that the mode has a significant field in the center cell, proved that the problem of low Q was solved.

The dependence of Q_0 on the accelerating gradient E was measured for the accelerating mode in the CW regime. Forward, reflected, and transmitted power levels (P_f, P_r, P_t), in addition to the Q_L at low power measured before, gave us more than enough data to calculate Q_0 and E. Hence, four different methods were used with a goal of estimating measurement errors by comparing the methods. In one of the methods, we used P_t to calculate energy stored in the cavity, and P_f and P_r to calculate Q_0.[23] In the other 3 methods, we ignored one of the 3 measured powers (P_f, P_r, or P_t), and replaced the ignored data with a calculation based on the other two powers and the assumption that Q_{ext} stayed constant throughout the experiment.

Figure 5 shows Q_0 vs E obtained using the four methods together with their average with error bars based on the differences between the methods. The point at $E = 4.6$ MV/m in Figure 5 corresponds to the expected value of Q_0 (listed in Table III) assuming no Q-degradation, and the accelerating gradient estimate based on the available RF power and measured losses in the transmission lines. The expected accelerating gradient was not achieved, possibly because of standing wave patterns in the transmission lines that may have limited the RF power fed into the cavity.

At low power, the obtained value of Q_0 was 1.55×10^8 (Figure 5), close to the expected value 1.81×10^8. As forward power was increased, some minimal conditioning was performed. At maximum available RF power, an accelerating gradient of (3.0 ± 0.3) MV/m was achieved. Using the ratios of the cavity's peak surface fields to the accelerating gradient from Table I, the maximum achieved surface fields were $E_{\text{surf}}^{\text{peak}} = (8.0 \pm 0.8)\,\text{MV/m}$ and $B_{\text{peak}}^{\text{surf}} = (13.4 \pm 1.3)\,\text{mT}$.

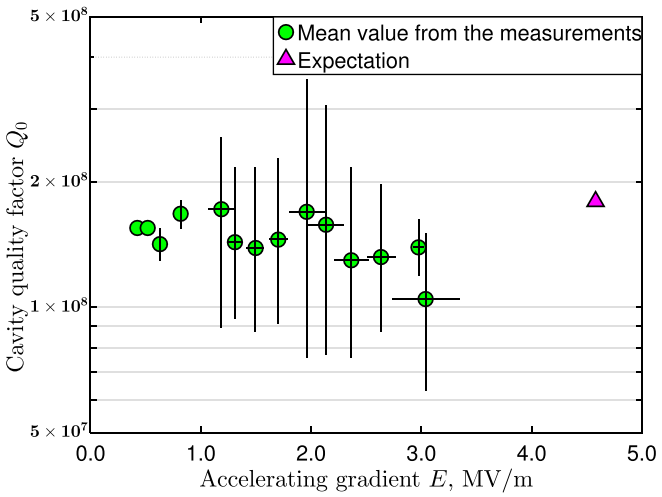

FIG. 5. Unloaded Q-factor and accelerating gradient in the accelerating mode, obtained during the second test at Niowave, Inc. The helium bath temperature was 4.2 K.

In summary, we presented the results of the cryogenic tests of the multi-cell SRF PBG cavity. No cavity leaks were observed during the tests in superfluid helium, proving the reliability of difficult electron-beam welding. The fact that the Q_0 for both the $\pi/5$ and the π modes agreed with the expectations indicated that the implemented surface treatment was effective in the cavity of such a complex shape. No hard barriers in the accelerating gradient were observed during the test, which indicated the absence of fundamental limits to the cavity's operation for a gradient of at least a few MV/m. The tested cavity is ready to be put in a complete cryomodule assembly, which is proposed as a prototype for the harmonic linac for the electron–relativistic-heavy-ion collider (eRHIC) at Brookhaven National Laboratory.[24]

This work was supported by a DOE Office of Nuclear Physics SBIR, Grant No. DE-SC0009523, the U.S. Department of Energy (DOE) Office of Science Early Career Research Program, and the DOE Office of High Energy Physics, Grant No. DE-SC0010075.

[1]M. W. Poole, S. I. Bennett, M. A. Bowler, N. Bliss, J. A. Clarke, D. M. Dykes, R. C. Farrow, C. Gerth, D. J. Holder, M. A. MacDonald *et al.*, in Proceedings of the Particle Accelerator Conference, Portland, OR, 2003, p. 189.
[2]T. Kasuga, T. A. Agoh, A. Enomoto, S. Fukuda, K. Furukawa, T. Furuya, K. Haga, K. Harada, S. Hiramatsu, T. Honda *et al.*, in Proceedings of the Particle Accelerator Conference, Albuquerque, New Mexico, 2007, Paper No. TUPMN044, p. 1016.
[3]G. H. Hoffstaetter, I. V. Bazarov, D. H. Bilderback, J. Codner, B. Dunham, D. Dale, K. Finkelstein, M. Forster, S. Greenwald, S. M. Gruner *et al.*, in Proceedings of the Particle Accelerator Conference, Albuquerque, New Mexico, 2007, Paper No. MOOBAB02, p. 107.
[4]M. Borland, G. Decker, A. Nassiri, and M. White, in Proceedings of the Particle Accelerator Conference, Albuquerque, New Mexico, 2007, Paper No. TUPMN089, p. 1121.
[5]E. C. Aschenauer, M. D. Baker, A. Bazilevsky, K. Boyle, S. Belomestnykh, I. Ben-Zvi, S. Brooks, C. Brutus, T. Burton, S. Fazi *et al.*, "eRHIC Design Study: An Electron-Ion Collider at BNL," (submitted).
[6]G. H. Hoffstaetter and I. Bazarov, Phys. Rev. Spec. Top.-Accel. Beams **7**, 54401 (2004).
[7]G. H. Hoffstaetter, I. V. Bazarov, and C. Song, Phys. Rev. Spec. Top. Accel. Beams **10**, 044401 (2007).
[8]S. Belomestnykh, Rev. Accel. Sci. Technol. **5**, 147 (2012).
[9]E. I. Smirnova, C. Chen, M. A. Shapiro, J. R. Sirigiri, and R. J. Temkin, J. Appl. Phys. **91**, 960 (2002).
[10]D. R. Smith, D. Li, D. C. Vier, N. Kroll, and S. Schultz, AIP Conf. Proc. **398**, 518 (1997).
[11]E. I. Smirnova, A. S. Kesar, I. Mastovsky, M. A. Shapiro, and R. J. Temkin, Phys. Rev. Lett. **95**(7), 074801 (2005).
[12]M. R. Masullo, M. Panniello, V. G. Vaccaro, A. Andreone, E. Di Gennaro, F. Francomacaro, G. Lamura, V. Palmieri, and D. Tonini, in Proceedings of the European Particle Accelerator Conference, 2006, p. 454, No. MOPCH167.
[13]E. I. Simakov, W. B. Haynes, M. A. Madrid, F. P. Romero, T. Tajima, W. Tuzel, C. H. Boulware, and T. L. Grimm, Phys. Rev. Lett. **109**, 164801 (2012).
[14]E. I. Simakov, S. A. Arsenyev, W. B. Haynes, D. Yu. Shchegolkov, N. A. Suvorova, T. Tajima, C. H. Boulware, and T. L. Grimm, Appl. Phys. Lett. **104**, 242603 (2014).
[15]S. A. Arsenyev, R. J. Temkin, D. Yu. Shchegolkov, E. I. Simakov, C. H. Boulware, T. L. Grimm, and A. R. Rogacki, Phys. Rev. Accel. Beams (submitted).
[16]S. A. Arsenyev, W. B. Haynes, D. Yu. Shchegolkov, E. I. Simakov, T. Tajima, C. H. Boulware, T. L. Grimm, and A. R. Rogacki, in Proceedings of SRF, Whistler, Canada, 2015, Paper No. WEA2A02, p. 1.

[17]T. Tajima, K. C. D. Chan, R. L. Edwards, R. C. Gentzlinger, W. B. Haynes, J. P. Kelley, F. L. Krawczyk, J. E. Ledford, M. A. Madrid, D. I. Montoya *et al.*, in Proceedings of SRF, Tsukuba, Japan, 2001, Paper No. PH002, p. 578.
[18]ANSYS, Ansys Inc., see www.ansys.com.
[19]H. Padamsee, J. Knobloch, and T. Hays, *RF Superconductivity for Accelerators*, 2nd ed. (Wiley-VCH), Chap. 4.7, p. 88.
[20]B. Piosczyk, P., Kneisel, O. Stoltz, and J. Halbritter, IEEE Trans. Nucl. Sci. **20**, 108 (1973).
[21]W. Hartung, J. Bierwagen, S. Bricker, J. Colthorp, C. Compton, T. L. Grimm, S. Hitchcock, F. Marti, L. Saxton, and R. C. Yorkl, in Proceedings of SRF, Lübeck/Travemünder, Germany, 2003, Paper No. TUP14, p. 313.
[22]L. Monaco, P. Michelato, C. Pagani, and N. Panzeri, in Proceedings of EPAC, Edinburgh, Scotland, 2006, Paper No. MOPCH170, p. 463.
[23]H. Padamsee, J. Knobloch, and T. Hays, *RF Superconductivity for Accelerators*, 2nd ed. (Wiley-VCH), Chap. 8.7, p. 160.
[24]S. Belomestnykh, I. Ben-Zvi, Y. Hao, V. Litvinenko, V. Ptitsyn, and W. Xu, in Proceedings of IPAC, Dresden, Germany, 2014, Paper No. TUPME084, p. 1547.